Online ISSN 1848-3380, Print ISSN 0005-1144
ATKAFF 57(3), 736–748(2016)

Toufik Roubache, Souad Chaouch, Mohamed-Saïd Naït-Saïd

Backstepping design for fault detection and FTC of an induction motor drives-based EVs

DOI 10.7305/automatika.2017.02.1733
UDK 681.511.4.015.44.037.09-047.82:[621.313.333:629.3-83]

Original scientific paper

This paper proposes an improved sensorless fault-tolerant control (FTC) for high-performance induction motor drives (IMD) that propels an electric-vehicle (EV). The design strategy is based on the Backstepping control (BC). However an appropriate combination of the BC and extended kalman filter (EKF) is done, this later is designed in order to detect and reconstruct the faults and also to give a sensorless control. Then, additional control laws, based on the estimates of the faults, are designed in order to compensate the faults. The results show the superiority EKF in nonlinear system as it provides better estimates for faults detection. A classical EV traction system is studied, using an IMD. Indeed, the IMD based powertrain is coupled to DC machine-based load torque emulator taking into account the EV mechanics and aerodynamics. Finally, the effectiveness of the proposed strategy for detection of faults, and FTC of the IMD is illustrated through simulation studies.

Key words: Backstepping control (BC), Fault-tolerant control (FTC), Induction motor drives (IMD), Extended kalman filter (EKF), Electric vehicle (EV).

Rekurzivna izvedba za uočavanje kvarnih stanja i upravljanje otporno na kvarna stanja električnih vozila zasnovanih na indukcijskim motorima. U ovome radu predložena je unaprijeđena bez-senzorska upravljačka strategija otporna na kvarna stanja (FTC) za indukcijski motor visokih performansi koji pokreće električno vozilo (EV). Strategija je temeljena na rekurzivnom upravljanju (BC). Nadalje, izvedena je odgovarajuća kombinacija BC-a i proširenog Kalmanovog filtra (EKF), pri čemu je potonji izveden u svrhu uočavanja i rekonstrukcije kvarova te kako bi omogućio bez-senzorsko upravljanje. Kako bi se kompenzirala kvarna stanja, dizajnirani su dodatni upravljački zakoni zasnovani na estimaciji kvarova. Rezultati prikazuju poboljšanje korištenjem EKF-a za nelinearne sustave budući da on omogućava kvalitetnije uočavanje kvarova. Razmatran je klasični pogon EV-a korištenjem IMD-a. Također, pogonski sklop zasnovan na IMD-u je povezan s emulatorom momenta zasnovanom na DC motoru, uzimajući u obzir mehaničke i aerodinamičke karakteristike EV-a. Na posljetku je simulacijama ilustrirana efikasnost predložene strategije za uočavanje kvarnih stanja i FTC-a IMD-a.

Ključne riječi: Rekurzivno upravljanje (BC), upravljanje otporno na kvarna stanja (FTC), indukcijski motor (IMD), prošireni kalmanov filtar (EKF), električno vozilo (EV).

1 INTRODUCTION

A motor control system with high robustness is an important issue in research. Induction motor drives (IMD) are making significant inroads, because of robustness and rugged structure. They are widely used in industrial applications such as, electric vehicles (EVs), traction locomotives etc. In the last decade, fault tolerance becomes an interesting topic in their controls. The objective is to give solutions that provide fault accommodation to the most frequent faults and thereby reduce the costs of handling the faults.

Backstepping control (BC) is a robust control for nonlinear systems. Based on the Lyapunov stability tools, this approach offers great flexibility in the synthesis of the regulator and naturally lends itself to an adaptive extension to the case. This control technique offers good performance in both steady state and transient operations, even in the presence of parameter variations and load torque disturbances.

Generally, the fault information, such as where the fault is and how bad the fault is, can be very useful information in designing a fault tolerant controller.

In recent years various researches have been done in the field of motor fault detection and fault tolerant control. Actually, fault-tolerant control concepts are divided into "passive" and "active" approaches [1-3]. Assuming the possible faults are known a priori, the passive method takes into account of all these possible faults in the design stage and

does not change the controller when the fault occurs [2-4]. An active method usually uses a fault detection and isolation (FDI) unit to collect the fault information and changes the controller according to the fault [5, 6]. Depending on the fault severity, a new control structure is applied, after the fault has been detected and reconstructed. Within this framework, the main goal of FTC is to improve the reliability of the system, which is rarely associated with an objective criterion that guides a design. In terms of control, FTC approach using Backstepping control is proposed, to improve the induction motor drive performances in case of rotor and stator failure. It does not consider whether the fault has occurred or not. The faults are considered as uncertainties and are taken into account in the controller design. A further objective consists to avoid the use of the speed and flux sensors. A wide variety of estimation techniques, have been used for the parameters and speed estimations. These approaches include the model reference adaptive system method [7, 8], speed observer method [9, 10] and the extended Kalman filter (EKF) [11, 12]. The EKF algorithm is an optimal recursive estimation algorithm for nonlinear systems. It processes all available measurements regardless of their precision, to provide a quick and accurate estimate of the variable of interest, and achieves rapid convergence.

In this work, the design of the fault tolerant controller for induction motors is based on the use of EKF for fault detection and reconstruction. Consequently, is considered to be the best solution for the speed and flux estimation using the measured state variables of an induction motor. On the other hand, a classical EV traction system is studied using a squirrel cage IMD. A separated excited DC load is thus controlled, to impose the same behavior of the mechanical power train to the IMD. Compared with the existing work already reported in the literature [13-21], the contributions of this paper are in the following aspects:

- The combination of the Backstepping control and the EKF to design a sensorless fault tolerant control scheme for IMD in presence of the faults.
- The EKF is used to detect, reconstruct the faults and to estimate the state of an IM model, and for sensorless control.
- The exploitation of an observer (EKF) to actively counteract the effect of faults.
- The proposed of an architecture emulating the electric vehicle dynamics.
- This study is to propose a new control strategy to improve dynamic performance of the traction motor in the EVs.

The outline of this paper is as follows. Section 2 defines the control problem and describes the nonlinear system. The dynamic model of EV and the nonlinear model of induction motor in presence of faults is explains in section 3. Then, the sensorless Backstepping control based fault detection and reconstruction are presented in Section 4. The proposed fault tolerant control strategy is described in Section 5. Section 6 is devoted to the presentation of the simulation results obtained for various fault-free situations and fault scenarios when the proposed scheme is applied to the IMD. Finally, some concluding remarks are given in Section 7.

2 STATEMENT OF THE PROBLEM

Let us consider a nonlinear uncertain system described as follows [21]:

$$\begin{cases} \dot{x} = f(x) + Bu + V_f \\ y = Cx \end{cases} \tag{1}$$

where $f(x)$ is smooth nonlinear function represents the nonlinear input uncertainty of the system, $x \in \Re^n$ is the measurable state vector, $u \in \Re^m$ is the control input, V_f is the control law designed for the faulty model, $V_f \in \Re^n$, y is the detectable state vector and B, C are known real constant matrices with appropriate dimensions.

The control input u is defined by:

$$u = u_{nom} + u_{ad} \tag{2}$$

When there are no actuator faults in (2), the additional control laws ($u_{ad} = 0$), so the control input becomes:

$$u = u_{nom} \tag{3}$$

To achieve the above control objectives under a wide range of faulty conditions, we propose in this work a robust control, namely Backstepping control (BC). The objective of the proposed approach is to design a robust nonlinear controller. To achieve this goal, and to avoid the use of speed and flux sensors, an extended kalman filter (EKF) observer is introduced to estimate the state of IM in the two cases, healthy and faulty conditions. The observer converges in a finite time and leads to good estimates of the flux and the speed even in the presence of faults, the rotor and stator resistance variations, and the load torque disturbance.

The proposed flexible fault tolerant architecture is illustrated in Figure 1. An alarm indicator is added to the system. The alarm signal will indicate that maintenance is needed if the fault is very big, then an alarm is sounded.

The proposed approach is applied to the traction system, which will be developed in the following section.

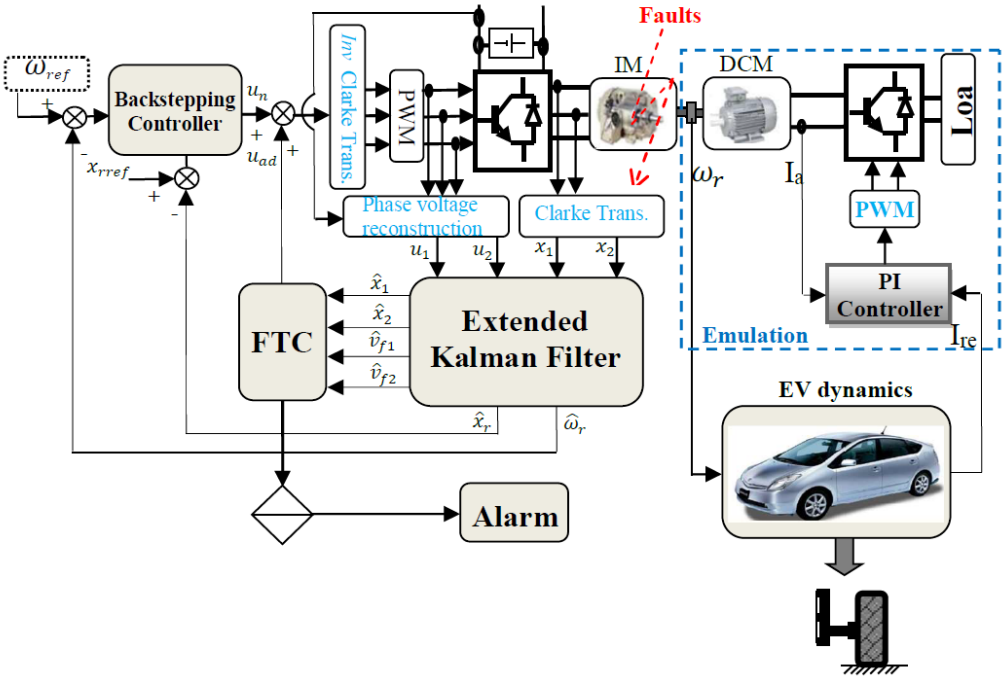

Fig. 1: The proposed fault tolerant control.

3 MODELING OF THE TRACTION SYSTEM

3.1 Modeling and dynamics of the EV

The traction drive is composed of a voltage source inverter supplying a squirrel cage induction motor (Fig.2), EV model and contact law between the wheel and the road are taken into account for dynamic modeling. However, the slip phenomenon is complex and requires specific controllers for good dynamic performance [22].

The road load is given by [23]:

$$F_w = F_{ad} + F_{ro} + F_{pr} + F_{\mathrm{sf}} \tag{4}$$

with F_{ad} is the aerodynamic drag force, F_{ro} is the rolling resistance force, F_{pr} is the profile force of the road, and F_{sf} is the Stokes or viscous friction force.

The vehicle velocity v_{ev} is obtained using the classical dynamics relationship with the traction and road load forces, F_t and F_w [24]:

$$M_{ev}\frac{dv_{ev}}{dt} = F_t - F_w \tag{5}$$

With M_{ev} is the mass of the electric vehicle.

The mechanical equation (in the motor referential) used to describe each wheel drive is expressed by:

$$J_{tm}\frac{d\omega_m}{dt} = T_m - T_B - T_{\mathrm{L}} \tag{6}$$

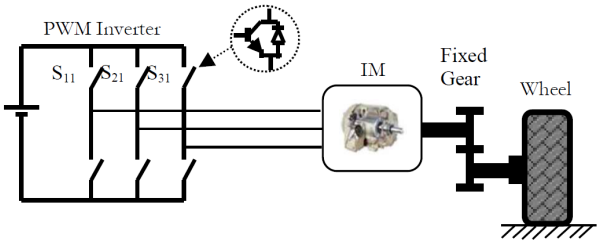

Fig. 2: Traction system scheme of the EV.

Where J_{tm} is the moment of inertia, T_m is the motor torque, T_B is the load torque accounting for friction and windage, and T_{L} is the load torque.

The gearbox leads to the gearbox torque T_{W} and the rotation speed ω_{W} given by:

$$\begin{cases} T_W = N\eta_{tr}T_m \\ \omega_W = \frac{\omega_m}{N} \end{cases} \tag{7}$$

The load torque is then given by:

$$T_L = \frac{T_{LW}}{N} = \frac{R_W F_W}{N} \tag{8}$$

where N is the transmission ratio, η_{tr} is the transmission efficiency, and R_{W} is the wheel radius.

The EV load torque emulator is based on DC machine (DCM) fed by a 4-quadrant chopper to control the generated current. Figure 1 shows then the proposed architecture emulating the EV dynamics.

3.2 Faulty Model of the Induction Motor

The model of the induction motor in the stationary reference frame with presence of faults is given by [19, 25]:

$$\dot{x} = f(x) + Bu + \gamma \mathrm{V_f} \tag{9}$$

with:

$$\begin{cases} \gamma = \begin{bmatrix} 1 & 0 & 0 & 0 \\ 0 & 1 & 0 & 0 \end{bmatrix}^T \\ \mathrm{V_f} = [\mathrm{V_{f1}} \quad \mathrm{V_{f2}}]^T \end{cases} \tag{10}$$

$$f(\mathrm{x}) = \begin{bmatrix} f_1(\mathrm{x}) \\ f_2(\mathrm{x}) \\ f_3(\mathrm{x}) \\ f_4(\mathrm{x}) \end{bmatrix} = \begin{bmatrix} \mathrm{a_1 x_1 + a_2 x_3 + a_3 \omega_r x_4} \\ \mathrm{a_1 x_2 - a_3 \omega_r x_3 - a_2 x_4} \\ \mathrm{a_4 x_1 + a_5 x_3 - \omega_r x_4} \\ \mathrm{a_4 x_2 + \omega_r x_3 + a_5\ x_4} \end{bmatrix} \tag{11}$$

where:

$$\begin{cases} [x_1 \ \ x_2 \ \ x_3 \ \ x_4.]^T = [i_{s\alpha} \ \ i_{s\beta} \ \ \varphi_{r\alpha} \ \ \varphi_{r\beta}.]^T \\ B = \begin{bmatrix} \mathrm{b_1} & 0 & 0 & 0 \\ 0 & \mathrm{b_2} & 0 & 0 \end{bmatrix}^T \\ u = [\mathrm{u_1} \ \ \mathrm{u_2}]^T = [v_{s\alpha} \ \ v_{s\beta}]^T \end{cases} \tag{12}$$

For simplicity, we define the following variables:

$$\begin{cases} \mathrm{a_1} = -\left(\frac{1}{\nabla T_s} + \frac{1-\nabla}{\nabla T_r}\right), \mathrm{a_2} = -\beta T_r, \mathrm{a_3} = \frac{M}{\nabla L_s L_r} \\ \mathrm{a_4} = M T_r, \mathrm{a_5} = -T_r, \mathrm{b_1} = \mathrm{b_2} = \frac{1}{\nabla L_s} \end{cases} \tag{13}$$

where $\nabla = 1 - \frac{M^2}{L_s L_r}$ is the coefficient of dispersion. L_s, L_r, M are stator, rotor and mutual inductance, respectively. R_s, R_r are respectively stator and rotor resistance. $T_s = \frac{L_s}{R_s}, T_r = \frac{L_r}{R_r}$ are respectively stator and rotor time constant.

The fault scenario considered in this paper addresses mechanical faults caused both by rotor and stator failures of the IM.

The presence of the faults generates asymmetry of the IM yielding some slot harmonics in the stator winding. In the two-phase model, it is possible to model this effect thinking of a sinusoidal component, which corrupts the stator currents:

$$\sum_i^{n_f} A_i \sin(\omega_i t + \varphi_i) \text{ and } \sum_i^{n_f} A_i \cos(\omega_i t + \varphi_i)$$

These assumptions allow us to express the deviation of the stator currents values in presence of faults values as:

$$\begin{cases} \mathrm{x_1} \to \mathrm{x_1} + \sum_i^{n_f} A_i \sin(\omega_i t + \varphi_i) \\ \mathrm{x_2} \to \mathrm{x_2} + \sum_i^{n_f} A_i \cos(\omega_i t + \varphi_i) \\ i = 1, ..., n_f \end{cases} \tag{14}$$

with n_f is faults number,

$$\omega_i = 2\pi f_i + 2\pi f_a = 2\pi(f_i + f_a) \tag{15}$$

where f_i is the characteristic frequency of the fault and f_a is the fundamental frequency.

In added $f_i = (1 \pm 2k\frac{s_a}{\omega_s})$ with $s_a = \omega_s - \omega_r$ is the slip angular frequency. k, ω_s are respectively positive integer and stator angular frequency.

In the induction motor, the presence of faults shows harmonic components on the stator currents with known frequency and unknown amplitude and phase. The frequency dependent on the kind of fault, which belongs to the two possible classes (rotor or stator faults). In (14), the amplitude A_i and phase φ_i are unknown values depended on the faults severity [26].

We define the exosystem by:

$$\dot{Z} = +\mathrm{S_f} Z \tag{16}$$

with:

$$\begin{cases} S_f = \mathrm{diag(S_{fi})} \\ \mathrm{S_{fi}} = \begin{bmatrix} 0 & \omega_i \\ -\omega_i & 0 \end{bmatrix} \\ \mathrm{z} = \begin{bmatrix} z_{2i-1} \\ z_{2i} \end{bmatrix}, i = 1, ..., n_f \end{cases} \tag{17}$$

The additive perturbing terms in (14), is considered as a suitable combination of the exosystem state, namely:

$$\begin{aligned} \mathrm{x_1} &\to \mathrm{x_1} + Q_d Z \\ \mathrm{x_2} &\to \mathrm{x_2} + Q_q Z \end{aligned} \tag{18}$$

with:

$$\begin{cases} Q_d = [1 \ \ 0 \ \ 1 \ \ 0...1 \ \ 0] \\ Q_q = [0 \ \ 1 \ \ 0 \ \ 1...0 \ \ 1] \end{cases} \tag{19}$$

In this way the uncertainty on the amplitude and phase of the additive sinusoidal terms in the faulty condition reflects in that on the initial state of the exosystem, once the perturbing terms $Q_d Z$ and$Q_q Z$ are added, by deriving (18) the $(\mathrm{x_1} - \mathrm{x_2})$ dynamics modify as:

$$\begin{cases} \dot{\mathrm{x}}_1 = \mathrm{a_1 x_1 + a_2 x_3 + a_3 \omega_r x_4 +} \\ \qquad \mathrm{b_1 u_1 + a_1} Q_d Z + Q_d S_f Z \\ \dot{\mathrm{x}}_2 = \mathrm{a_1 x_2 + a_3 \omega_r x_3 - a_2 x_4 +} \\ \qquad \mathrm{b_2 u_2 + a_1} Q_q Z + Q_q S_f Z \end{cases} \tag{20}$$

Then the model of the IM in the presence of faults is given by (9) with exogenous input:

$$\begin{cases} \dot{x}_1 = \mathrm{a_1 x_1 + a_2 x_3 + a_3 \omega_r x_4 + b_1 u_1 + V_{f1}} \\ \dot{x}_2 = \mathrm{a_1 x_2 - a_3 \omega_r x_3 - a_2 x_4 + b_2 u_2 + V_{f2}} \\ \dot{x}_3 = \mathrm{a_4 x_1 + a_5 x_3 - \omega_r x_4} \\ \dot{x}_4 = \mathrm{a_4 x_2 + \omega_r x_3 + a_5 x_4} \end{cases} \tag{21}$$

With:

$$\begin{cases} \mathrm{V_{f1}}= \mathrm{a_1 Q_d Z + Q_d S_f Z} \\ \mathrm{V_{f2}}= \mathrm{a_1 Q_q Z + Q_q S_f Z} \end{cases} \tag{22}$$

This equation is rewritten as follows:

$$\begin{cases} V_f = -\begin{bmatrix} \mathrm{a_1}Q_d + Q_d S_f \\ \mathrm{a_1}Q_q + Q_q S_f \end{bmatrix} \\ \Gamma = \begin{bmatrix} \Gamma_1 \\ \Gamma_1 \end{bmatrix} = \begin{bmatrix} [\mathrm{a_1}Q_d + Q_d S_f] \\ [\mathrm{a_1}Q_q + Q_q S_f] \end{bmatrix} \end{cases} \tag{23}$$

4 SENSORLESS BACKSTEPPING CONTROL OF INDUCTION MOTOR

4.1 Backstepping Control

The backstepping control offered numerous advantages such as, achievement a high precision; ensure good stability of the system and good transient performance. The proposed control technique has high performance in transient and permanent regimes. The basic idea of this approach is to render the equivalent closed-loop system to stable subsystems by Lyapunov theory [27-29].

Before applying this approach, we need to define a new variable representing the square of the rotor flux.

$$\begin{aligned} &\varphi_r = \mathrm{x_3} + j\mathrm{x_4} \\ &= \left(\mathrm{x_3^2} + x_4^2\right)^{1/2} \left(\cos(\theta_s) + j\sin(\theta_s)\right) \end{aligned} \tag{24}$$

The rotor position is defined by the angle θ_s given by:

$$\theta_\mathrm{s} = \arctan\left(\frac{\mathrm{x_4}}{\mathrm{x_3}}\right) \tag{25}$$

We consider the square of the rotor flux:

$$x_r = \varphi_\mathrm{r}^2 = \mathrm{x_3^2 + x_4^2} \tag{26}$$

According to (9) and (11), its derivative is given by:

$$\begin{aligned} &\dot{x}_r = 2\left(x_3\dot{x}_3 + x_4\dot{x}_4\right) \\ &= -2\mathrm{T_r}x_r + 2\mathrm{T_r\ M}\left(\mathrm{x_1 x_3 + x_2 x_4}\right) \end{aligned} \tag{27}$$

The synthesis of this control is achieved in two successive steps:

First Step

We define two errors e_1 and e_2 representing respectively, the error between the real speed ω_r and reference speed ω_{ref} and the error between the square of the rotor flux and its reference x_{ref}.

$$\begin{cases} e_1 = \omega_\mathrm{ref} - \omega_\mathrm{r} \\ e_2 = x_\mathrm{ref} - x_\mathrm{r} \end{cases} \tag{28}$$

The derivative of (28) is given by:

$$\begin{cases} \dot{e}_1 = \dot{\omega}_{ref} - \frac{\rho}{J}(x_2 x_3 - x_1 x_4) + \frac{T_L}{J} \\ \dot{e}_2 = \dot{x}_\mathrm{ref} + 2T_\mathrm{r}x_r - 2MT_r(x_1 x_3 + x_2 x_4) \end{cases} \tag{29}$$

In order to check the tracking performances, we choose the first Lyapunov candidate functionV_1 associated with the rotor flux and speed errors, such as:

$$V_1 = \frac{1}{2}(e_1^2 + e_2^2) \tag{30}$$

Using Eq. (29), the derivative of Eq. (30) is written as follows:

$$\begin{aligned} &\dot{V}_1 = (e_1\dot{e}_1 + e_2\dot{e}_2) \\ &= e_1(\dot{\omega}_{ref} - \tfrac{\rho}{J}(x_2 x_3 - x_1 x_4) + \tfrac{T_L}{J}) + e_2(\dot{x}_\mathrm{ref} + 2T_\mathrm{r}x_r \\ &-2MT_r(x_1 x_3 + x_2 x_4) \end{aligned} \tag{31}$$

Thus, the tracking objectives will be satisfied if we choose:

$$\begin{cases} x_{1ref} = \frac{\mathrm{J}}{\rho \mathrm{x_4}}(k_1 e_1 + \dot{\omega}_\mathrm{ref} + \\ \qquad \frac{T_L}{J}) + \frac{1}{2\mathrm{T_r Mx_3}}(k_2 e_2 + \dot{x}_\mathrm{r} + 2\mathrm{T_r}x_r) \\ x_{2ref} = \frac{\mathrm{J}}{\rho \mathrm{x_3}}(k_1 e_1 + \dot{\omega}_\mathrm{ref} + \\ \qquad \frac{T_L}{J}) + \frac{1}{2\mathrm{T_r Mx_4}}(k_2 e_2 + \dot{x}_\mathrm{r} + 2\mathrm{T_r}x_r) \end{cases} \tag{32}$$

Therefore, (31) can be rewritten as:

$$\dot{V}_1 = (-k_1 e_1^2 - k_2 e_2^2) < 0 \tag{33}$$

where k_1 and k_2 are positive design constants that determine the closed loop dynamics.

According to (33), the controls $x_{1\mathrm{ref}}$and$x_{2\mathrm{ref}}$in (32) are asymptotically stabilizing.

Second Step

In this step, we define other errors in the components of the stator currents and their references. Let us recall the current errors, such as:

$$\begin{cases} e_3 = x_{2\mathrm{ref}} - x_2 \\ e_4 = x_{1\mathrm{ref}} - x_1 \end{cases} \tag{34}$$

So the dynamics of$e_1$and e_2 are written:

$$\begin{cases} \dot{e}_1 = -k_1 e_1 - \frac{\rho}{J}(e_4 x_4 - e_3 x_3) \\ \dot{e}_2 = -k_2 e_2 + 2MT_r(e_4 x_3 - e_3 x_4) \end{cases} \tag{35}$$

From (34), (9) and (11), the derivative errors dynamics in (33) are given by:

$$\begin{cases} \dot{e}_3 = \dot{x}_{2ref} - \delta_1 - b_2 u_2 \\ \dot{e}_4 = \dot{x}_{1ref} - \delta_2 - b_1 u_1 \end{cases} \tag{36}$$

with:

$$\begin{cases} \delta_1 = -\mathrm{a_1 x_2} - \mathrm{a_3}\omega_\mathrm{r}\mathrm{x_3} + \mathrm{a_3 T_r x_4} \\ \delta_2 = -\mathrm{a_1 x_1} - \mathrm{a_3 T_r x_3} + \mathrm{a_3}\omega_\mathrm{r}\mathrm{x_4} \end{cases} \tag{37}$$

In this step we define the control laws, while final Lyapunov function based on all the errors of the speed, the rotor flux and the stator currents, such as:

$$V_1 = \frac{1}{2}(e_1^2 + e_2^2 + e_3^2 + e_4^2) \tag{38}$$

Its derivative with respect to time is:

$$\dot{V}_2 = (e_1\dot{e}_1 + e_2\dot{e}_2 + e_3\dot{e}_3 + e_4\dot{e}_4) \tag{39}$$

According to (34) and (35), this equation can be rewritten as follows:

$$\begin{aligned}\dot{V}_2 = &-k_1e_1^2 - k_2e_2^2 + \\ &e_3(\dot{x}_{2ref} - \delta_1 - b_2u_2 - 2MT_rx_4 + \tfrac{\rho}{J}x_3e_1) + \\ &e_4(\dot{x}_{1ref} - \delta_2 - b_1u_1 + 2MT_rx_3e_2 - \tfrac{\rho}{J}x_4e_1)\end{aligned} \tag{40}$$

The stator voltages control is, then deduced as follows:

$$\begin{cases} \mathrm{u}_1 = \frac{1}{\mathrm{b}_1}(\dot{x}_{1ref} + k_4e_4 - \delta_2 + 2MT_r\mathrm{x}_3e_2 - \frac{\rho}{J}\mathrm{x}_4e_1) \\ \mathrm{u}_2 = \frac{1}{\mathrm{b}_2}(\dot{x}_{2ref} + k_3e_3 - \delta_1 + 2MT_r\mathrm{x}_4e_2 + \frac{\rho}{J}\mathrm{x}_3e_1) \\ k_3 > 0, k_4 > 0 \end{cases} \tag{41}$$

Then, (36) can be expressed as:

$$\begin{cases} \dot{e}_3 = -k_3e_3 - \frac{\rho}{J}x_3e_1 - 2MT_rx_4e_2 \\ \dot{e}_4 = -k_4e_4 + \frac{\rho}{J}x_4e_1 - 2MT_rx_3e_2 \end{cases} \tag{42}$$

The choice of k_3 and k_4 as positive parameters can made $\dot{V}_2 < 0$.

To show boundedness of all states, we can rearrange the dynamical equations from (35) and (42) as:

$$\begin{bmatrix} \dot{e}_1 \\ \dot{e}_2 \\ \dot{e}_3 \\ \dot{e}_4 \end{bmatrix} = \mathrm{H} \begin{bmatrix} e_1 \\ e_2 \\ e_3 \\ e_4 \end{bmatrix} \tag{43}$$

where:

$$\mathrm{H} = \begin{bmatrix} e_1 & 0 & \frac{\rho}{J}x_3 & -\frac{\rho}{J}x_4 \\ 0 & -k_2 & -2MT_rx_4 & 2MT_rx_3 \\ -\frac{\rho}{J}x_3 & -2MT_rx_4 & -k_3 & 0 \\ \frac{\rho}{J}x_4 & -2MT_rx_3 & 0 & -k_4 \end{bmatrix} \tag{44}$$

In Eq. (43), the matrix H can be shown to be Hurwitz, this proves the boundedness of all the states.

4.2 EKF as Faults Estimation and Speed Observer

This section considers the use of extended kalman observer for fault detection and reconstruction. EKF is employed to estimate the motor state variables by only using the measurements of stator voltages and currents [30]. EKF uses errors estimation signal for the estimation of faults and states.

The discrete IMD state model used by the EKF is developed in the stationary reference frame and summarized by:

$$\begin{cases} x(k+1) = g(x(k), u(k)) + \omega(k) \\ y(k+1) = h(x(k+1)) + v(k) \end{cases} \tag{45}$$

where $\omega(k)$ and $v(k)$ are white Gaussian noise processes with covariance matrices $Q(k)$ and $R(k)$, but the covariance matrix of noise vector, which is shown below:

$$cov(w) = E\{ww^T\} = Q, cov(v) = E\{vv^T\} = R$$

According to equations (9) and (11) with$V_f \neq 0$, the matrix g and h are given by:

$$\begin{cases} \mathrm{g(k)} = \begin{bmatrix} (1-\mathrm{T_e a_1})\mathrm{x_1} + \mathrm{T_e a_2 x_3} \\ \quad + \mathrm{T_e a_3 x_4 \omega_r} + \mathrm{T_e b_1 u_1} \\ -\lambda_1 \tanh Z_{y1} \\ (1-\mathrm{T_e a_1})\mathrm{x_2} - \mathrm{T_e a_5 x_3 \omega_r} \\ \quad + \mathrm{T_e a_6 x_4} + \mathrm{T_e b_2 u_2} \\ -\lambda_2 \tanh Z_{y2} \\ \mathrm{T_e a_4 x_1} + (1-\mathrm{T_e a_5})\mathrm{x_3} - \mathrm{T_e x_4 \omega_r} \\ \mathrm{T_e a_4 x_2} + \mathrm{T_e x_3 \omega_r} + (1-\mathrm{T_e a_5})\mathrm{x_4} \end{bmatrix} \\ h(k) = Cx_{(k/k+1)} \end{cases} \tag{46}$$

The predicted covariance matrix is estimated by:

$$P(k+1/k) = F(k)P(k)F(k)^T + Q \tag{47}$$

The Kalman gain matrix is obtained by:

$$K(k+1) = P(k+1/k)C^T\left[CP(k+1/k)C^T + R\right]^{-1} \tag{48}$$

The error covariance matrix is obtained by:

$$P(k+1/k+1) = P(k+1/k)\left[I_n - CK(k+1)\right] \tag{49}$$

The estimated speed is considered as a variable parameter. A global observer structure can be written as:

$$\dot{\hat{x}} = f(\hat{x}) + Bu + K(y - \hat{y}) - \lambda u_{ad} \tag{50}$$

with:

$$\begin{cases} y = [\,x_1 \;\; x_2\,]^T \\ \lambda = [\,\lambda_1 \;\; \lambda_2\,]^T \\ u_{ad} = [\,u_{ad1} \;\; u_{ad2}\,]^T \end{cases} \tag{51}$$

K is the observer gain matrix which is selected to insure the error stability.

The global adaptive flux and speed observer structure is illustrated in figure (3). Then the speed adaptive mechanism is given by:

$$\hat{\omega}_r = K_p(z_1\hat{x}_4 - z_2\hat{x}_3) + K_i\int(z_1\hat{x}_4 - z_2\hat{x}_3)\,dt \tag{52}$$

where $z_1 = (x_3 - \hat{x}_3)$ and $z_2 = (x_4 - \hat{x}_4)$, K_p, K_i are positive gains.

Thus, the speed value is estimated by a simple PI controller, to minimize the error:

$$\varepsilon = (z_1\hat{x}_4 - z_2\hat{x}_3) \tag{53}$$

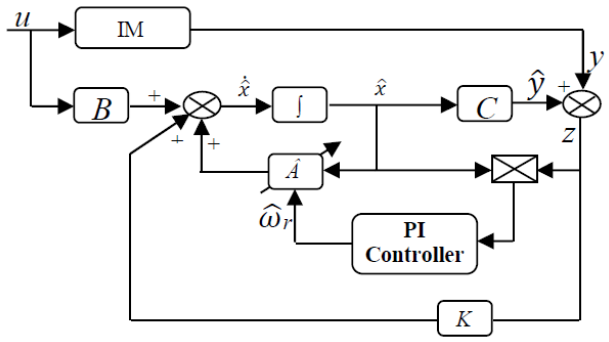

Fig. 3: Adaptive observer structure.

5 PROPOSED FAULT-TOLERANT STRATEGY AND LOAD DRIVE CONTROLLER

A fault-tolerant system is a system able to detect the presence of faults and being able to maintain stability and better performance capabilities of the system [32]. The additive control ($u_{ad} = \hat{V}_f$) is added to the nominal control to compensate the faults effect (FTC aspect). It assumes that the effects of faults on the system can be adequately modeled by an exogenous signal from a stable autonomous system called exosystem [33]. The IMD will be evaluated using a controlled load drive. This load drive has to impose the same rotation speed as imposed by the mechanical power train (EV dynamics). To provide the right set point to the DC machine (DCM) rotation speed, the mechanical model is used with the IMD torque as input.

The fault tolerant architecture proposed in this paper is illustrated in figure (1). The objective of this technique is to provide an observer (EKF) that generates an additive term u_{ad} in the absence of faults that are added to the nominal control to compensate the effect of faults on the system.

The instantaneous difference between the derivative of the system state and the estimated system becomes:

$$\dot{\tilde{Z}}_x = \begin{bmatrix} \dot{\hat{x}}_1 \\ \dot{\hat{x}}_2 \\ \dot{\hat{x}}_3 \\ \dot{\hat{x}}_4 \end{bmatrix} - \begin{bmatrix} \dot{x}_1 \\ \dot{x}_2 \\ \dot{x}_3 \\ \dot{x}_4 \end{bmatrix} \tag{54}$$

$$\dot{\tilde{Z}}_x = 0 \Leftrightarrow \begin{cases} (1-a_1)\,\tilde{z}_{x1} - \lambda_1 \tanh z_{y1} - V_{f1} = 0 \\ (1-a_1)\,\tilde{z}_{x2} - \lambda_2 \tanh z_{y2} - V_{f2} = 0 \\ -a_4 \tilde{z}_{x1} + (1-a_5)\,\tilde{z}_{x3} - \\ \qquad (\hat{\omega}_r - \omega_r)\,\tilde{z}_{x4} = 0 \\ -a_4 \tilde{z}_{x2} - (\hat{\omega}_r - \omega_r)\,\tilde{z}_{x3} + \\ \qquad (1-a_5)\,\tilde{z}_{x4} = 0 \end{cases} \tag{55}$$

Equation (55) shows that z_x converges to zero, as $t \to \infty$, then $\hat{\omega}_r \to \omega_r$.

Thus, the fault is estimated by the following expression:

$$\begin{cases} \hat{V}_{f1} = -\lambda_1 \tanh z_{y1} \\ \hat{V}_{f2} = -\lambda_2 \tanh z_{y2} \end{cases} \tag{56}$$

The function tanh represent a hyperbolic function. λ_1 and λ_2 are selected constant vector, $(z_{y1} = \hat{y}_1 - y_1)$ and $(z_{y2} = \hat{y}_2 - y_2)$ are the output estimation errors.

5.1 Reconfiguration Strategy

The structure of the global proposed fault tolerant controller is given by:

$$u = \begin{bmatrix} u_1 \\ u_2 \end{bmatrix} = \begin{bmatrix} u_{1nom} \\ u_{2nom} \end{bmatrix} + \begin{bmatrix} u_{1ad} \\ u_{2ad} \end{bmatrix} \tag{57}$$

With u_{1nom} and u_{2nom} are the backstepping control laws, they are designed in un-faulty mode $(V_f = 0)$ to steer the tracking errors to zero and to compensate the load disturbance. u_{1ad} and u_{2ad} are additional control laws (compensation units) that will be designed in order to compensate the effect of faults.

Finally, the objective of the control is achieved by adopting the performed procedure and may compensate the effect of faults on the system.

In the case of global control reconfiguration, the additional control laws (u_{1ad} and u_{2ad}) can be expressed by:

$$\begin{cases} u_{1ad} = -\frac{1}{b_1}\hat{V}_{f1} \\ u_{2ad} = -\frac{1}{b_2}\hat{V}_{f2} \end{cases} \tag{58}$$

6 NUMERICAL SIMULATION AND DISCUSSION

Numerical simulation results are presented in this section to validate the efficiency of the proposed FTC scheme. The overall block diagram of the induction motor drive is shown in Fig. 1. A Matlab/Simulink computer program was developed to model the whole system. The parameters of simulations have been carried-out for an electric vehicle using a 1.5 kW induction motor with squirrel cage rotor based powertrain, supplied by a 3-leg VSI and a 1 kW separated excited DC machine supplied by a 4-quadrant chopper. The model of EV consists of a mass of 1.5 t, a wheel radius of 0.3 m, and a vehicle width of 1.6 m. The adaptation coefficients are chosen in function of speed and torque limitations: $N = 20$. The nominal parameters values of the used induction motor are shown in Table 1.

Three cases are simulated. In the first case, we have illustrated the response of the machine without faults. In the second case there is one fault affect the motor in the stator caused by stator asymmetries (static eccentricity). In the third case there are two faults affects the motor in the stator (static eccentricity) and rotor (dynamic eccentricity).

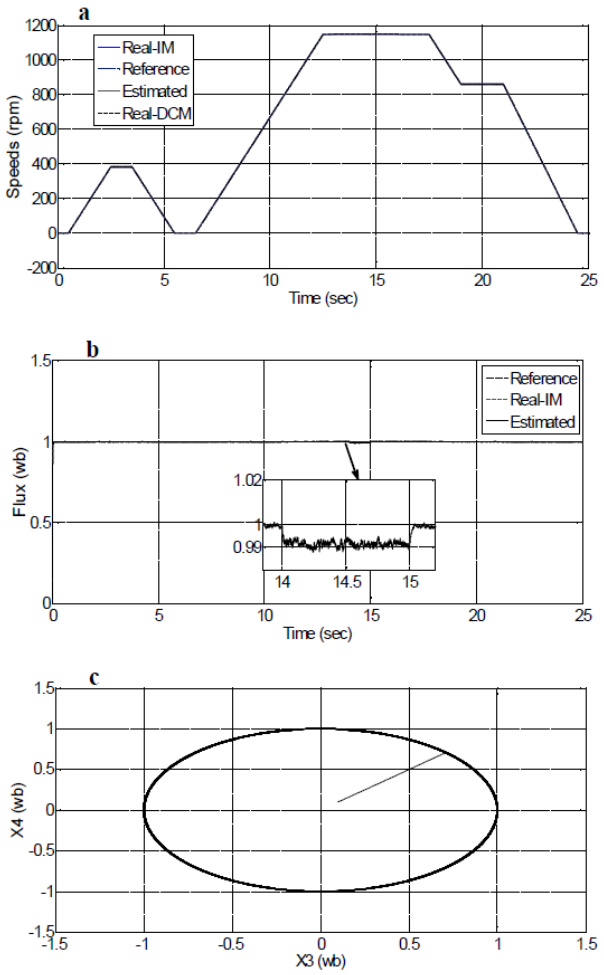

Fig. 4: Simulation responses of an IM under 100% variations of *Rs* and *Rr*, applied at time $t = 14\,\mathrm{s}$. From upper to lower plots: Speeds, flux (reference, real and estimated) and tracking flux, where IM via backstepping controller.

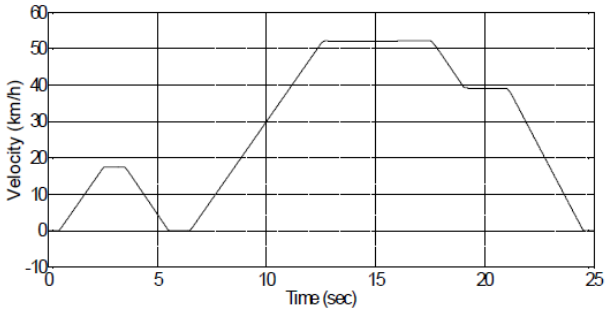

Fig. 5: Emulated vehicle velocity.

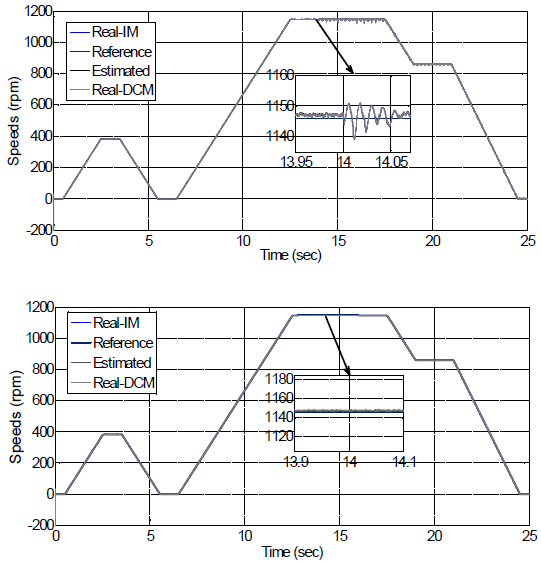

Fig. 6: Reference, real and estimated of IM and DCM speeds in faulty conditions (upper plot) in case of single fault affect the IM at time $t = 14\,\mathrm{s}$, and healthy conditions (lower plot) with using the proposed FTC scheme.

6.1 Simulation of the Backstepping control case

The first objective of this case is to evaluate the IM performance in healthy mode. In this case, variations of 100% of the rotor resistance (R_r) and stator resistance (R_s) between the time $t = 14\,\mathrm{s}$ and $t = 15\,\mathrm{s}$ with variable speed reference are introduced.

Fig. 4 shows the motor speeds (a), the rotor flux trajectory (b), and the flux linkage (c).

We notice that the responses of speed and flux shows that the influence of this variation is weak, and that the dynamic error of flux and of speed estimation always remains low. We can see that the control present a stable and acceptable response.

6.2 Single fault case

The obtained results are shown in Figures 5 to 10. It is concluded from the simulations that, besides the rejection of external disturbance in all results. Thus, it clear to see that, the proposed FTC system gives satisfactory results in term of stability and tracking performance for the IMD. Then at time t= 14s an occurrence of one fault in the stator (Static eccentricity) is provoked. A trapezoidal trajectory with a reverse operation is imposed as set point of the vehicle velocity. The rotor speed of the machine converges to the speed generated by the mechanical model.

The simulation results show that the proposed FTC strategy is able to maintain the vehicle stability and acceptable performance under both faulty and fault free conditions.

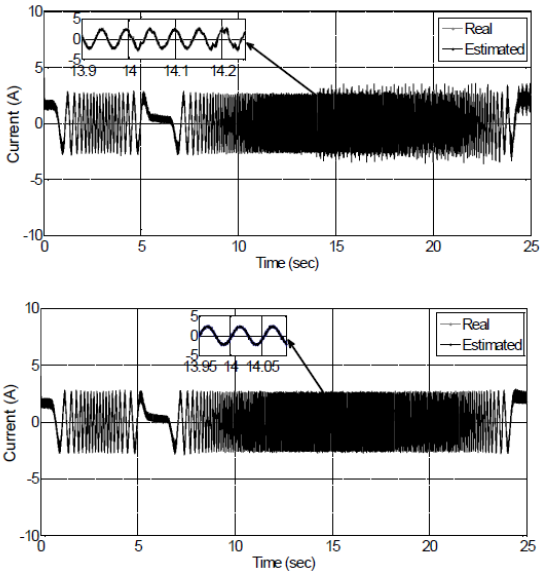

Fig. 7: Induction motor currents (x_2) in faulty conditions (upper plot) case of single fault affect the IM at time $t = 14\,\mathrm{s}$, and healthy conditions (lower plot) with using the proposed FTC scheme.

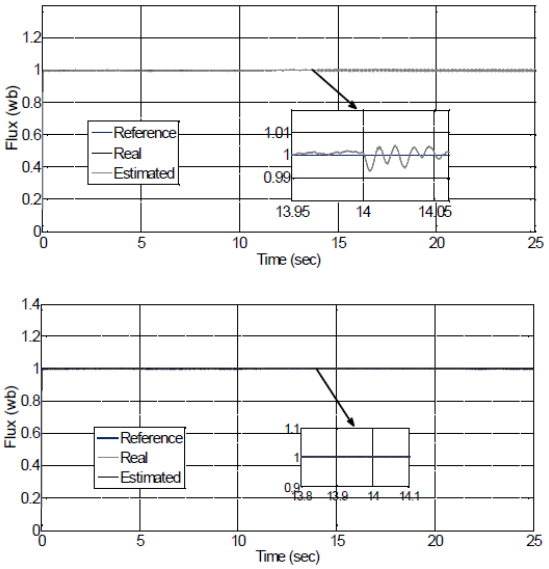

Fig. 8: Induction motor reference, real and estimated rotor flux in faulty conditions (upper plot) in case of single fault affect the IM at time $t = 14\,\mathrm{s}$, and healthy conditions (lower plot) with using the proposed FTC scheme.

Fig. 7 shows the IMD currents in both conditions. As we can see from the plots, an oscillatory behavior is observed when the fault is switched. Such oscillatory behavior can be easily eliminated by using the proposed fault tolerant control. We were able to achieve good tracking performances and disturbance rejection.

6.3 Two fault case

In this case, two faults are introduced, one in the stator and the other in the rotor. The same tests, presented previously, are applied to the machine during the introduction of fault tolerant control Figures (11-15).

The rotor flux and the speed follow up the reference quickly and perfectly for the backstepping control which confirms the robustness of this technique. In order to simulate the stator fault, figures 9 and 10 shows the EKF performance in the estimate of unknown additive faults *Vf1* and *Vf2*.

From these results, we can see that the proposed control is robust to parameter variations, but is insufficient in case of faults. Increased strength reduces the error on the speed but can not cancel the effect of faults on the currents.

The results show clearly the effectiveness of the FTC control that occurs during the application of the fault by removing all defects. In faulty conditions, it is found that EKF has better performance for high and low speeds and is also less sensitive to rotor and stator resistance variations.

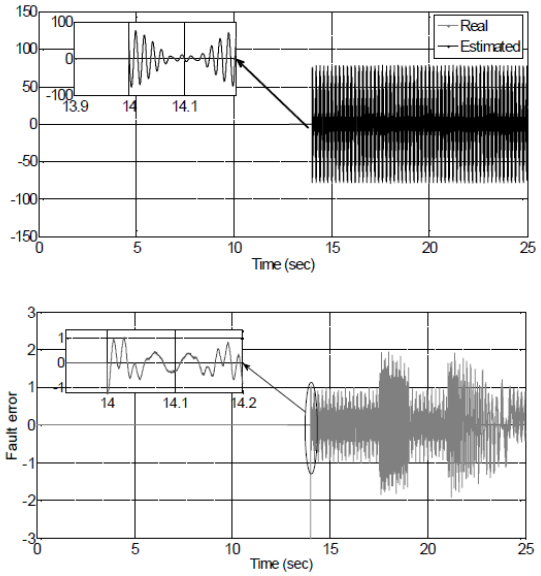

Fig. 9: Real and estimated fault in case of single stator fault (V_{f1}) affect the IM at time $t = 14\,\mathrm{s}$ (upper plot), and fault error (lower plot) when using the proposed FTC scheme.

7 CONCLUSION

In this paper, we have proposed a new improved sensorless fault-tolerant control around the Backstepping struc-

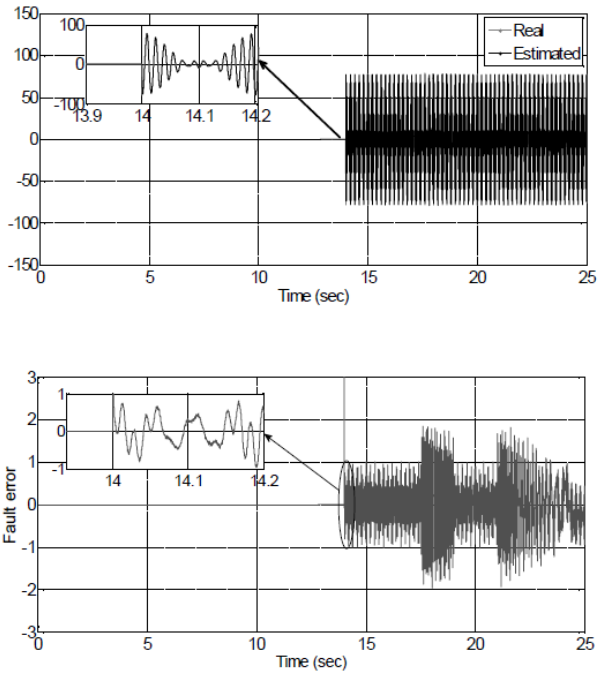

Fig. 10: Real and estimated fault in case of single stator fault (V_{f2}) affect the IM at time $t = 14\,\mathrm{s}$ (upper plot), and fault error (lower plot) when using the proposed FTC scheme.

ture for induction motor drive by using both Backtepping strategy and Lyapunov stability theory. A new approach to fault estimation is presented, where an EKF is used for a good estimation of the faults. Then, additional control laws based on the resulting faults estimates permit to eliminate the effect of the faults.

The effectiveness of the proposed FTC system is verified by controlling two mechanical systems, an induction motor and an electric vehicle. The simulation results prove that the proposed FTC scheme can guarantee the good tracking performance as well as the stability of the closed-loop system against the simulated faults. Finally, it is important to highlight that the final performances of the proposed FTC strategy are mainly due to the fault estimate.

APPENDIX A

Table 1. Rated data of the simulated Induction Motor

$1.5\,\mathrm{kW}$, $5\,\mathrm{Nm}$, $1430\,\mathrm{rpm}$, $p = 2$, $R_s = 5.72\Omega$, $R_r = 4.2\Omega$, $L_s = 0.462\,\mathrm{H}$, $L_r = 0.462\,\mathrm{H}$, $M = 0.44\,\mathrm{H}$, $J = 0.0049\,\mathrm{kg.m^2}$

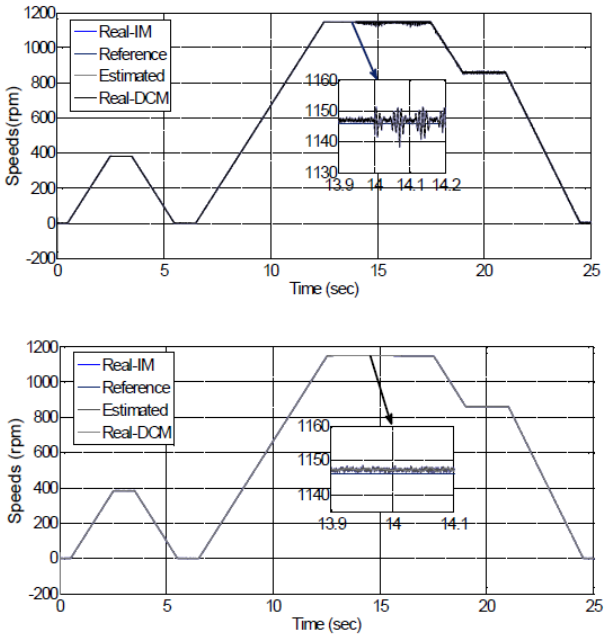

Fig. 11: Reference, real and estimated of IM and DCM speeds in faulty conditions (upper plot) in case of two faults affects the IM at time $t = 14\,\mathrm{s}$, and healthy conditions (lower plot) with using the proposed FTC scheme.

Table 2. Rated data of the simulated DC Machine

$1\,\mathrm{kW}$, $5\,\mathrm{Nm}$, $1500\,\mathrm{rpm}$, $R_a = 2.581\Omega$, $R_e = 281.3\Omega$, $L_a = 0.028\,\mathrm{H}$, $L_e = 156\,\mathrm{H}$, $J = 0.02215\,\mathrm{kg.m^2}$

REFERENCES

[1] Zidani F, Diallo D, Benbouzid M, Nait said R. A fuzzy based approach for the diagnosis of fault modes in a voltage-fed PWM inverter induction motor drive. IEEE Trans. Ind. Electron, 2008, vol. 55, 586-593.

[2] Jin X Z. Robust adaptive switching fault-tolerant control of a class of uncertain systems against actuator faults, Math. Probl.Eng, 2013, 1-9.

[3] Hwang I, Kim S, Kim Y, Seah C.E.A survey of fault detection, isolation, and reconfiguration methods. IEEE.Trans. Contr. Syst. Tech, 2010, vol. 18, 636-653.

[4] Bartolini G, Ferrara A, Levant F, et al.Variable structure systems, sliding mode and nonlinear control. Springer, 1999.

[5] Levant A. Universal Single-input-single-output (SISO) Sliding mode Controllers with Finite Time Convergence. IEEE Trans. On Automatic Control, 2001, 49(9):1447–1451.

[6] Harnefors L, Hinkkanen M. Complete stability of reduced-order and full-order observers for sensorless IM drives.

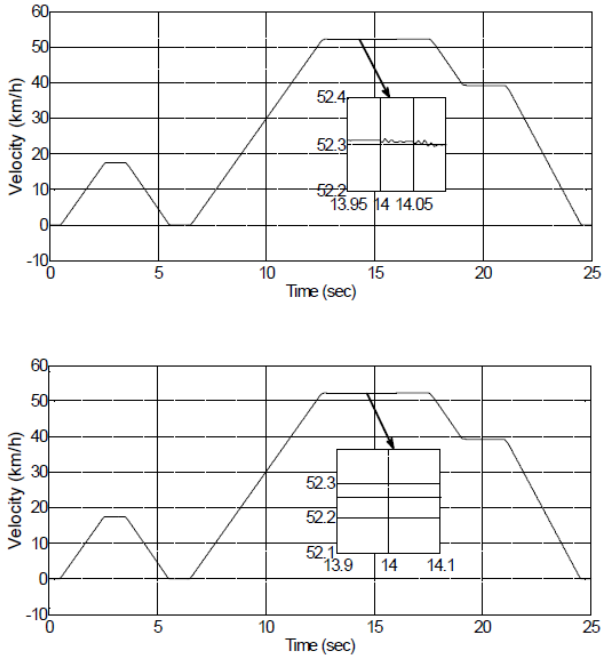

Fig. 13: Emulated vehicle velocity in case of two faults affects the IM at time $t = 14\,\mathrm{s}$ (upper plot), and healthy conditions (lower plot) when using the proposed FTC scheme.

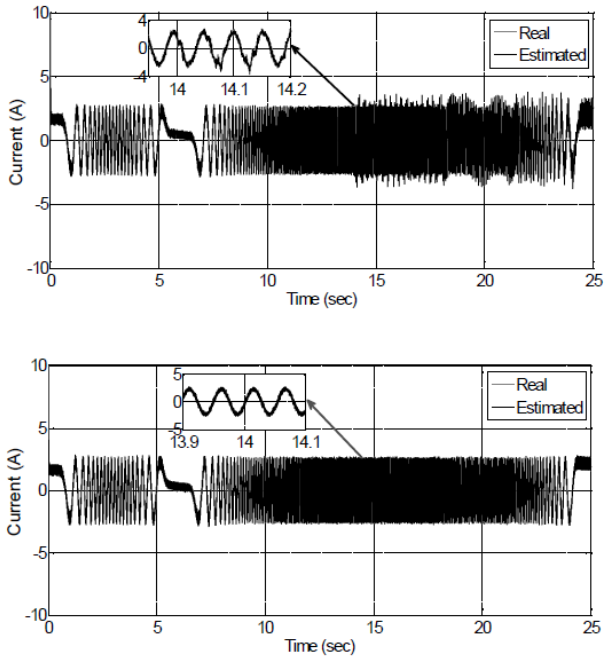

Fig. 14: Induction motor currents (x_1) in faulty conditions (upper plot) in case of two faults affects the IM at time $t = 14\,\mathrm{s}$, and healthy conditions (lower plot) with using the proposed FTC scheme.

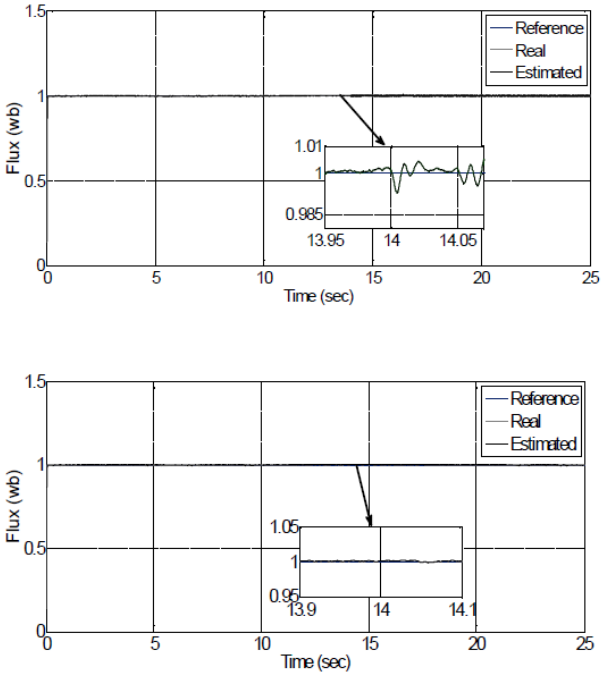

Fig. 12: Induction motor reference, real and estimated rotor flux in faulty conditions (upper plot) in case of two faults affects the IM at time $t = 14\,\mathrm{s}$, and healthy conditions (lower plot) with using the proposed FTC scheme.

IEEE Trans on Industrial Electronics 2008, 55(3):1319–1329.

[7] Uddin M N, Hao W, Rebeiro R S, Hafeez M. Experimental performance of a model referenced adaptive flux observer based NFC for IM drive. IEEE Industry Applications Society Annual Meeting, 2011,1–8.

[8] Ohara M, Noguchi T. Sensorless control of surface permanent-magnet motor based on model reference adaptive system. IEEE 9th International Conference on Power Electronics and Drive Systems, 2011, 608–614.

[9] Cirrincione M, Accetta A, Pucci M, Vitale G. MRAS speed observer for high performance linear induction motor drives based on linear neural networks. IEEE Transactions on Power Electronics, 2013, 28(1): 123–134.

[10] Guzinski J, Diguet M, Krzeminski Z, Lewicki A, Abu-Rub H. Application of speed and load torque observers in high-speed train drive for diagnostic purposes. IEEE Transactions on Industrial Electronics, 2009, 56(1):248–256.

[11] Khanesar M A, Kayacan E, Teshnehlab M, Kaynak O. Extended Kalman filter based learning algorithm for type-2 fuzzy logic systems and its experimental evaluation. IEEE Transactions on Industrial Electronics, 2012, 59(11): 4443–4455.

[12] Kim J H, Lee S S, Kim R Y, Hyun D S. A sensorless control using extended Kalman Filter for an IPM synchronous mo-

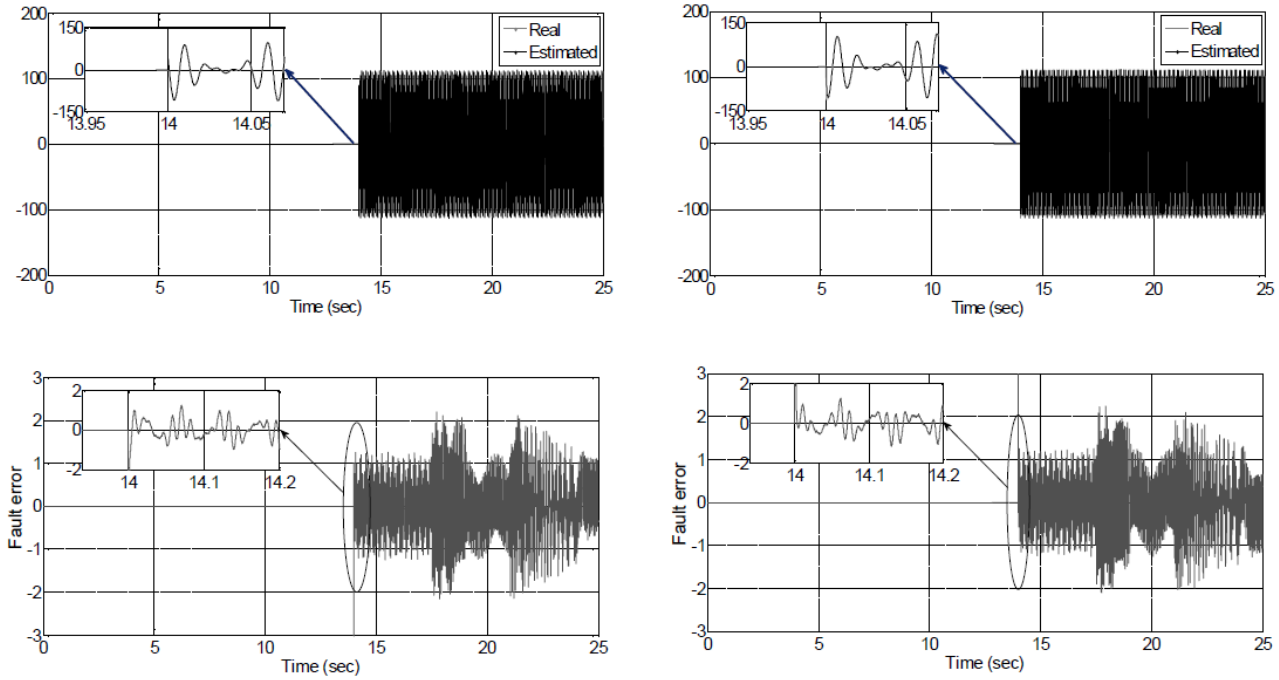

Fig. 15: Real and estimated fault (left upper plot), and fault error (left lower plot). Real and estimated fault (right upper plot), and fault error (right lower plot). All these results in case of two faults affects the IM at time $t = 14\,\mathrm{s}$, and with using the proposed FTC scheme.

tor based on an extended rotor flux. 38th Annual Conference on IEEE Industrial Electronics Society, 2012, 1631–1636.

[13] Paoli A, Marconi L, Bonivento C. A Fault-tolerant strategy for induction motors. Proceedings of the 40th IEEE Conference on Decision and Control Orlando, Florida USA, 2001.

[14] Bonivento C et *al.* Implicit fault-tolerant control: Application to induction motors. Automatica, 2004, vol. 40, 355-371.

[15] Edwards C, Pin Tan C. Sensor fault tolerant control using sliding mode observers. Control Engineering Practice 14, 2006, 897–908.

[16] Fekih A. Effective fault tolerant control design for nonlinear systems: application to a class of motor control system. IET Control Theory and Applications, 2008, 2(9): 762–772.

[17] Djeghali N, Ghanes M, Djennoune S, Barbot J. Sensorless Fault Tolerant Control for Induction Motors. International Journal of Control Automation and Systems, 2013, 11(3):563-576.

[18] Fekih A. Fault Diagnosis and Fault Tolerant Control Design for Aerospace Systems: A Bibliographical Review. American Control Conference (ACC), Portland, Oregon, USA, 2014.

[19] Roubache T, Chaouch S, Nait said MS . Backstepping fault tolerant control for induction motor. Power Electronics, Electrical Drives, Automation and Motion (SPEEDAM), Ischia, Italy, 2014.

[20] Shakouhi M, Mohamadian M, Afjei E. Fault-Tolerant Control of Brushless DC Motors Under Static Rotor Eccentricity.IEEE Transactions on Industrial Electronics, 2015, 62(3).

[21] Fekih A, Seelem S. Effective fault-tolerant control paradigm for path tracking in autonomous vehicles. Systems Science & Control Engineering: An Open Access Journal, 2015, 3(1): 177-188.

[22] Bouscayrol A, Lhomme W. Hardware-in-the-loop simulation of electric vehicle traction systems using Energetic Macroscopic Representation. IEEE IECON'06, Paris (USA), 2006.

[23] Moura S J, Fathy H K, Callaway D S, Stein J L. A stochastic optimal control approach for power management in plug-in hybrid electric vehicles. IEEE Trans. On Control Systems Technology, 2011, 19(3): 545–554.

[24] Roubache T, Kheloui A. Programmable emulator loading conditions of EV traction systems. JIEMCEM, Oran-Algeria, 2010.

[25] Roubache T, Chaouch S, Nait said MS. A fault-tolerant control for induction-motors using sliding mode scheme.14th International Conference on Sciences and Techniques of Automatic control & computer engineering - STA'2013 Sousse, Tunisia, 2013.

[26] Blodt M, Granjon P, Raison B, Regnier L. Mechanical Fault Detection in Induction Motor Drives Through Stator Current Monitoring-Theory and Application Examples. Author manuscript published in "Fault Detection, Wei Zhang", 2010, 451-488.

[27] H.T. Lee, L.C. Fu, and F.L. Lian, "Sensorless adaptive backstepping speed control of induction motor" .In *Proc IEEE Conference on Decision & Control, USA, December* 2002, pp. 1252-1257.

[28] H. Tan et *al.*, "Adaptive backstepping control of induction motor with uncertainties" .*In Proceedings of the IEEE ACC'99*, San Diago (USA), vol. 1, pp. 1-5, June 1999.

[29] I. K. Bousserhane, A. Hazzab, M. Rahli, B. Mazari, M. Kamli, "Position Control of Linear Induction Motor using an Adaptive Fuzzy Integral-Backstepping Controller". *Serbian journal of electrical engineering,* Vol. 3, no. 1, pp. 1-17, June 2006.

[30] Bose B K. Modern Power Electronics and AC drives. 3rd ed. Upper Saddle River, N J, Prentice Hall, 2003, 388-400 and 348-350.

[31] Alonge F, D'Ippolito F, Fagiolini A, Sferlazza A. Extended complex Kalman filter for sensorless control of an induction motor. Control Engineering Practice 27, 2014, 1-10.

[32] Harnefors L, Hinkkanen M. Complete stability of reduced-order and full-order observers for sensorless IM drives. IEEE Trans. On Industrial Electronics, 2008, 55(3):1319–1329.

[33] Muenchhof M et *al.* Fault-tolerant actuators and drives—Structures, fault detection principles and applications. Annual Reviews in Control, 2009.

Toufik Roubache was born in M'sila, Algeria, in 1982. He received the B.Sc. degree from the University of M'sila, Algeria, in 2005, and the M.Sc. degrees from Military Polytechnic School, Algiers, Algeria, in 2008, all in Electrical Engineering. He is currently working toward the Ph.D. degree in Electrical Engineering at the University of Batna, Algeria. His research interests include the robust sensorless fault tolerant control of electrical drives.

Souad Chaouch was born in Batna, Algeria, in 1969. She received the B.Sc. degree in Electrical Engineering, from the University of Batna, Algeria, in 1993, and the M.Sc . degree in Electrical and automatic Engineering from the same university in 1998, She received her Ph.D. degree in 2005. She has been with the University of Msila, Algeria between 2000 and 2011. Currently, she is full Professor at the Electrical Engineering Institute at University of Batna, Algeria. She is a member in the Research Laboratory of Electromagnetic Induction and Propulsion Systems of Batna University. Her scientific research include electric machines and drives, automatic controls, Sensorless Controls and Non linear controls.

Mohamed-Saïd Naït-Saïd was born in Batna, Algeria, in 1958. He received the Engineer Diploma in Electrical Engineering from the National Polytechnic High School of Algiers, Algeria in February 1983, and the MSc degree in Electronics and Control Engineering from Electronics department of Constantine University in 1992. He received the Phd degree in Electrical Engineering from University of Batna after its free scientific researches accomplished in Automatic Laboratory of Amiens University in French from 1996 to 1999. Currently he is a full professor at the Electrical Engineering Department of Batna University II and assures the chief of the Master course of Control and Diagnosis of the Electrical Systems. From 2000-2005, Dr. Naït-Saïd was the head of the first created research laboratory in Batna University, named Electromagnetic Induction and Propulsion Systems (LSPIE) of Batna and also in 2006 the head of scientific committee of the same department. LSPIE has been evaluated by the Algerian ministry of the universities as the best laboratory in Batna University (100 percent satisfactory). Dr. Naït-Saïd has supervised twenty five Masters and ten Phd thesis. His research interests include the electric machines and their control drives and diagnosis.

AUTHORS' ADDRESSES

Mr Toufik Roubache, Master
University of Msila, Electrical Engineering Department
Email: toufik_roubache@yahoo.com

Prof. Souad Chaouch, Ph.D.
Prof. Mohamed-Saïd Naït-Saïd, Ph.D.
Laboratory of Electromagnetic Induction and Propulsion Systems
University of Batna,
Route de Biskra, Batna, 05000, Algeria
Email: chaouchsouad@yahoo.fr, medsnaitsaid@yahoo.fr

Received: 2016-03-18
Accepted: 2016-06-07